Bioelectrochemistry 82 (2011) 112–116

Contents lists available at ScienceDirect

Bioelectrochemistry

journal homepage: www.elsevier.com/locate/bioelechem

# Direct electrochemistry and electrocatalysis of myoglobin-based nanocomposite membrane electrode

Yancai Li *, Yuanjun Li, Yiyun Yang

*Chemistry Department of Zhangzhou Normal University, N36 Zhangzhou, Zhangzhou, 363000, PR China*

ARTICLE INFO

*Article history:*
Received 12 April 2011
Received in revised form 24 April 2011
Accepted 15 June 2011
Available online 24 June 2011

*Keywords:*
Multi-wall carbon nanotubes
Chitosan
Myoglobin
Silver nanoparticles
Biosensor

ABSTRACT

The direct electron transfer of myoglobin (Mb) was achieved based on the immobilization of Mb/Silver nanoparticles (AgNPs) on glassy carbon electrode by multi-wall carbon nanotubes (MWNTs)-chitosan(Chit) film. The immobilized Mb displayed a pair of well-defined and reversible redox peaks with a formal potential ($E^{\theta'}$) of −24 mV (vs. Ag/AgCl) in 0.1 M pH 7.0 phosphate buffer solution. The apparent heterogeneous electron transfer rate constants ($k_s$) of Mb confined to Chit-MWNTs film was evaluated as 5.47 $s^{-1}$ according to Laviron's equation. The surface concentration ($\Gamma^*$) of the electroactive Mb in the Chit-MWNTs film was estimated to be $(4.16 \pm 0.35) \times 10^{-9}$ mol $cm^{-2}$. Meanwhile, the catalytic ability of Mb toward the reduction of $H_2O_2$ was studied. Its apparent Michaelis–Menten constant for $H_2O_2$ was 0.024 mM, showing a good affinity. The linear range for $H_2O_2$ determination was from $2.5 \times 10^{-5}$ M to $2.0 \times 10^{-4}$ M with a detection limit of $1.02 \times 10^{-6}$ M (S/N = 3). Moreover, the biosensor displays rapid response to $H_2O_2$ and good stability and reproducibility.



## 1. Introduction

The immobilization of metalloproteins is of great importance in developing practical biosensors or in mimicking electrocatalytic roles in living systems [1]. Nanoscale materials have been demonstrated to be an ideal matrix of protein immobilization in fabricating various biosensors, which greatly benefits from the ability to promote electron-transfer reactions and high thermal capacity, and efficiently retain the biological activity of proteins [2–4]. In recent years, nanocomposites have been applied in the biosensing and surface functionalizing, and have exhibited an enhanced performance owing to the synergistic effect [5].

Myoglobin (Mb), a kind of heme-contained redox proteins with a single chain of 153 amino acids, exists in mammalian skeleton and muscle tissues and functions in the storage of oxygen and in the enhancement of the rate of oxygen diffusion [6]. Heme proteins usually contain the porphyrin complex of iron (II) or hemin (III) as a prosthetic group. The iron atom in the center of heme porphyrin has six coordinate bonds, four of which participate in the coordination with the nitrogen atoms in porphyrin ring and form a plane. Meanwhile, the fifth coordinate bond links with the nitrogen atom in 93-imidazolyl of histidine along the axial direction. This structure hinders the response of Mb in conventional electrode, which is probably ascribed either to its three-dimensional structure or to its denaturation adsorption onto the surface of the electrode and subsequent passivation of the electrode surfaces. The introduction of nanoarchitectures could force Mb into an effective orientation for electron transfer, which helps maintain the bioactivity of the immobilized Mb and the biocatalytical activity of the biosensor [7]. Carbon nanotubes (CNTs), containing multi-walled carbon nanotubes (MWNTs) and single-walled carbon nanotube (SWNTs), have been widely used as immobilization matrix to fabricate various Mb-based sensors [8]. The matched interaction with Mb, resulted from quantum size effect of CNTs, can promote the orientation of Mb on the MWNTs or SWNTs and thus the electron transport. The excellent conductivity serves MWNTs or SWNTs on electrode as the extended electrode surfaces, which could greatly reduce the electron-transfer distance of Mb. Moreover, nanocomposites of CNTs and noble metal nanostructures, such as platinum nanoparticles, have been utilized to enhance the sensitivity of the biosensors, presumably due to the increased specific surface area, the improved conductivity and spatial structure [9]. However, reports on the composite membrane of MWNTs and silver nanoparticles (AgNPs) in smaller size are unavailable up to now. AgNPs are cheaper and easier to synthesize as compared with platinum nanoparticles. Also, the complex of MWNTs and AgNPs in smaller size may form some hierarchical-like nanostructures, which could ensure favorable orientation of Mb in the composite membrane and thus provide Mb an environment similar to the native microenvironment.

Chitosan is a natural polymer with abundant amino and hydroxyl groups, originated in chitin (sufficient in crustaceans) [10]. The chitosan not only serves as a membrane-forming agent, but plays a role of stabilizer and dispersant, owing to its desirable properties such as splendid film-forming, nontoxicity, chemical inertness, biological compatibility, and good adhesion. Furthermore, a Chit-MWNTs composite film could exhibit significant improvement in tensile modulus

* Corresponding author. Tel.: +86 596 2591445; fax: +86 596 2520035.
*E-mail address:* liyancai2000@yahoo.com.cn (Y. Li).

1567-5394/$ – see front matter © 2011 Elsevier B.V. All rights reserved.
doi:10.1016/j.bioelechem.2011.06.004

and strength as compared to neat chitosan film [11] or MWNTs film [12]. Hence, Mb-based composite membrane containing chitosan, MWNTs and AgNPs is desirable for an amperometric biosensor of $H_2O_2$.

In this study, we fabricated a nanocomposite film through casting Chit-MWNTs onto AgNPs-Mb modified electrode. The conformation of Mb immobilized in the composite film retained its native structure as characterized by ultraviolet visible (UV–vis) spectroscopy. The composite nanostructure promoted Mb to undergo a rapid, reversible and sensitive electron transfer process. Also, the Mb-based nanocomposite membrane electrode showed a good catalytic activity towards the reduction of $H_2O_2$. The high sensibility, good reproducibility, and long-term stability can serve the proposed electrode as an amperometric $H_2O_2$ biosensor.

## 2. Experimental

### 2.1. Reagents

Equine heart myoglobin (No. M-1882, type III) was purchased from Sigma Chemical Company and used as received. Chitosan (Deacetylation>95%) was obtained from Sanland Chemical Co. LTD. Both trisodium citrate dihydrate and sodium borohydride were purchased from Sinopharm Chemical Reagent Co. LTD. Silver nitrate was from Shantou xilong chemical factory Guangdong. The multi-wall carbon nanotubes (MWNTs, >95% purity) were purchased from Shenzhen nanoport Co. LTD. Stock solutions of $H_2O_2$ were freshly diluted from 30% solution (purchased from Shantou xilong Chemical Co. LTD). 0.1 M phosphate buffer solutions (PBS) with various pH values were prepared by mixing stock standard solutions of $Na_2HPO_4$ and $NaH_2PO_4$. A chitosan solution (1 wt.%) was prepared by dissolving 0.03 g chitosan in 3 mL acetic acid (v/v, 1%). All other chemicals were of analytical grade and were used without further purification. All solutions were made up with double-distilled water.

### 2.2. Apparatus

UV–vis spectra were recorded on a GBC Cintra $10_e$ UV—Visible spectrometer. The electrochemical experiments were carried out with a CHI 650 °C electrochemical workstation (CH Instruments, USA) with a conventional three-electrode cell. The modified or unmodified glassy carbon electrode was used as the working electrode. The Pt wire and Ag/AgCl (3.0 M KCl) electrode were used as the counter and reference electrodes, respectively. Cyclic voltammetric measurements were performed in a static cell while amperometric experiments were carried out in a stirred system. All solutions were purged with high-purity nitrogen for at least 20 min prior to experiments and a nitrogen environment was then kept over the solution in the cell. All experiments were performed at a temperature of $20 \pm 2$ °C. Aliquots of hydrogen peroxide solution were added successively to the solution in amperometric experiments. Current-time data were recorded after a steady-state current had been achieved.

### 2.3. Preparation of AgNPs

All glassware used in the procedures was firstly washed with freshly prepared $HNO_3$/HCl (1:3, v/v), then rinsed thoroughly with double-distilled water and dried prior to use. Silver nanoparticles were prepared according to the literature [13] by using sodium citrate and sodium borohydride to reduce silver nitrate in a mixing solution. $AgNO_3$ and $Na_3$citrate solutions needed were filtered through a 22 μm microporous membrane filter prior to use. In brief, 1 mL of $AgNO_3$ was added to 90 mL of double-distilled water. After 1 min of stirring, 2 mL of sodium citrate (1 wt.%) was added. One minute later, 1 mL of fresh 0.075% $NaBH_4$ (prepared in the 1% sodium citrate solution) was added. The solution was stirred for an additional 5 min, poured into a brown glass bottle and stored at 4 °C. The electronic absorption peak of the silver nanoparticles prepared is about 390 nm in the visible region. The average nanoparticle diameter is $8 \pm 2.4$ nm as measured by transmission electron microscopy (not shown here).

### 2.4. Preparation of Chit-MWNTs/Mb/AgNPs/GC electrode

Glassy carbon electrode (3 mm-diameter) were polished first with 1.0-, 0.3-, 0.05-μm alumina slurry. After rinsing thoroughly with double-distilled water, they were sonicated in absolute ethanol and double-distilled water for about 1 min, respectively. Then GCE was cycled in the potential range between 0.4 and −0.4 V at 100 mV $s^{-1}$ for 2 cycles in 6 mL of 5 mM $K_3[Fe(CN)_6]$. Upon putting 24 mg of MWNTs into 3 mL of a chitosan solution (1wt.%), ultrasonic agitation for a few minutes gave a black suspension. Mb solution was obtained by dissolving 6.0 mg of Mb in 3 mL of 0.1 M pH 7.32 PBS, and the AgNPs were used as prepared. Then 20 μL mixture of Mb and AgNPs (v/v = 1:1) was dropped onto the surface of a cleaned glassy carbon electrode with a microsyringe and allowed to dry at 4 °C for 24 h. After the GCE was cooled, it was smeared evenly with 20 μL of a Chitosan-MWNTs (1 wt.%) solution by a microsyringe, and then dried at a temperature of 4 °C for another 24 h. The solvent was allowed to evaporate before use. The final electrode was taken as the Chit-MWNTs/Mb/AgNPs/GCE. The similar procedures were employed to fabricate the Chit-MWNTs/AgNPs/GCE and Chit-MWNTs/Mb/GCE. All resulting electrodes were stored at 4 °C when not in use.

A 0.1 M phosphate buffer solution (pH 7.0) was used as supporting electrolyte for the determination of hydrogen peroxide. Before and after every measurement, the Chit-MWNTs/Mb/AgNPs/GCE was activated by successive cyclic voltammetric sweeps between −0.3 V and 0.5 V at 100 mV $s^{-1}$ in a blank phosphate buffer solution (pH 7.0).

## 3. Results and discussion

### 3.1. UV–vis characterization

The Soret band of heme protein is usually an indicator of the microenvironment where the heme center locates. This peak will be shifted if the protein is denaturated. The band for native Mb in solution is located at 406 nm according to the literature [8] reported previously. Fig. 1 shows the UV–vis absorption spectra of Mb solution and Chit-MWNTs/Mb/AgNPs, respectively. As seen from Fig. 1b, dry films of Chit-MWNTs/Mb/AgNPs on quartz slides have a characteristic Soret absorption band at 408 nm, the same as that of native state of Mb in solution (Fig. 1a). The accordance indicates that Mb keeps its natural structure in the dry films of Chit-MWNTs/Mb/AgNPs and not denatured.

### 3.2. Direct electrochemistry of Mb

Fig. 2 shows the cyclic voltammograms of different electrodes in 0.1 M pH 7.0 PBS at 100 mV $s^{-1}$. A couple of well-defined redox peaks could be observed on the Chit-MWNTs/Mb/AgNPs/GCE, as shown in Fig. 2d, while no peak appeared at a bare GCE (Fig. 2a) or Chit-MWNTs/AgNPs/GCE (Fig. 2b). Obviously, the response of Chit-MWNTs/Mb/AgNPs/GCE was attributed to the redox process of the electroactive center of the immobilized Mb. Its anodic peak potential ($E_{pa}$) and the cathodic peak potential ($E_{pc}$) were located at 15 and −39 mV (vs. Ag/AgCl), respectively, with the formal potential of −0.012 V (vs. Ag/AgCl) and the peak separation of 54 mV (vs. Ag/AgCl). This electrochemical reaction corresponded to the reversible conversion between Mb–Fe (III) and Mb–Fe (II) [14]. Furthermore, a comparative experiment was carried out for Mb entrapped in the Chi-MWNTs film in the absence of AgNPs. A lower and less reversible faradic response was obtained at the Chit-MWNTs/Mb/GCE (Fig. 2c) than at the Chit-MWNTs/Mb/AgNPs/GCE. Thus, we can conclude that the electron transfer of Mb can be

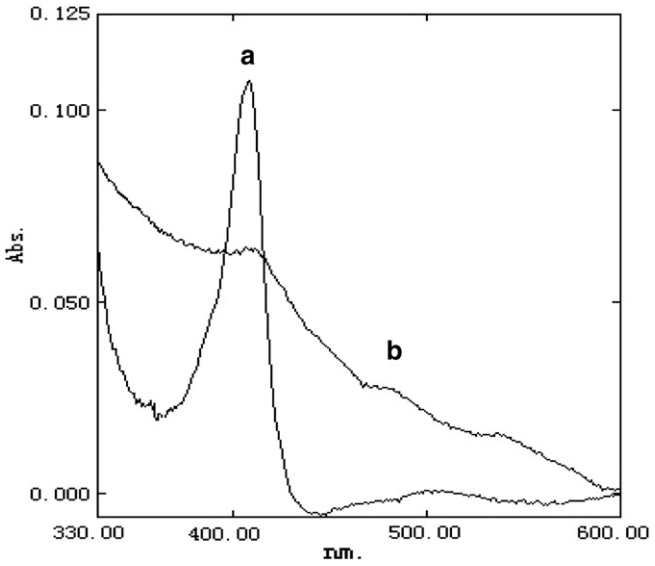


**Fig. 1.** UV–Vis absorption spectra of (a) pure myoglobin solution (2 mg $mL^{-1}$) and (b) the Chit-MWNTs/Mb/AgNPs film on quartz slides.

further enhanced by silver nanoparticles when mixing with carbon nanotubes although the latter also showed the ability of enhancing it. The improvement could be ascribed to the synergistic effect of MWNTs and AgNPs on facilitating the electron transport of Mb. Firstly, the complex of MWNTs and AgNPs may form some hierarchical-like nanostructures, which could greatly increase the specific surface area for the adsorption of Mb as compared with single MWNTs. Secondly, the silver nanoparticles could be matched to Mb in size. Mb could have an effective orientation for electron transfer on the Chit-MWNTs/AgNPs, presumably due to the quantum size effect and high surface curvature of silver nanoparticles as well as the hierarchical-like structure of the complex. Thirdly, the efficient conducting tunnel formed by MWNTs and AgNPs and the membrane-forming function of chitosan have the Chit-MWNTs/AgNPs film suitable to immobilize Mb for the investigation of electron transport. Therefore, the favorable microenvironment help ensure the rapid, reversible, sensitive and stable electron transfer of Mb in the Chit-MWNTs/Mb/AgNPs film.

Fig. 3 shows the CVs of Chit-MWNTs/Mb/AgNPs/GCE in pH 7.0 PBS at different scan rates. As shown in Fig. 4, both the cathodic and anodic peak currents were almost symmetrical and linearly proportional to the scan rate in the range from 10 to 500 mV $s^{-1}$. The linear regression equations are expressed as $I_{pc}$ (μA) = (2.43 ± 0.03) + (0.11 ± 0.001)v (mV $s^{-1}$) (R = 0.998) and $I_{pa}$ (μA) = −(2.42 ± 0.01) − (0.11 ± 0.002)v (mV $s^{-1}$) (R = 0.998), respectively. This result indicates that the electrochemical behavior of Mb immobilized in Chit-MWNTs/AgNPs-modified films is a surface-controlled process. Moreover, the cathodic peak potential almost unchanged with the increasing scan rate, indicating that all the electroactive ferric myoglobin [Mb–Fe (III)] in the film was reduced to ferrous myoglobin [Mb–Fe (II)] in the cathodic scan and that the Mb–Fe (II) produced was reoxidized to Mb–Fe (III) in the reverse scan. The high reaction efficiency could result from the large specific surface area, the effective orientation of Mb and the efficient conductivity in the Chit-MWNTs/Mb/AgNPs film. For such a surface process, the average surface coverage ($\Gamma^*$) can be calculated according to the Laviron Equation [15].

$$I_p = n^2F^2vA\Gamma^* / 4RT = nFQv / 4RT \quad (1)$$

where $v$ is the scan rate, $A$ is the effective surface area of the modified electrode, $I_p$ is the peak current, $Q$ is the quantity of charge, $n$ is the number of electron transferred in the electrode reaction, $R$ is mol gas constant, $F$ is Faraday constant, and $T$ is the temperature (298.15 K). From the slope of $I_p$–$v$ curve, $\Gamma^*$ of Mb on Chit-MWNTs/Mb/AgNPs/GCE was estimated to be $(4.16 \pm 0.35) \times 10^{-9}$ mol $cm^{-2}$, which is larger than that of Konjac Glucomannan films modified GCE ($4.61 \times 10^{-11}$ mol $cm^{-2}$) [16]. It is suggested that a multilayer of proteins participated in the electron transfer process of the composite dry films.

According to the method of Laviron [15], taking charge transfer coefficient($\alpha$) as 0.5 and a scan rate >200 mV $s^{-1}$ with peak separation ($E$p), the average value of electron transfer rate constant ($k_s$) was determined to be about 5.47 $s^{-1}$, confirming a reversible redox process of Mb at Chit-MWNTs/AgNPs-modified electrode. The value for electron transfer rate constant is higher than that of Mb immobilized in silver nanoparticles doped carbon nanotubes film, 0.41 $s^{-1}$ [17], and in Clay–chitosan–gold nanoparticle nanohybrid, 2.66 ± 0.15 $s^{-1}$ [18]. The excellent performance indicates that the electron transfer of Mb in Chit-MWNTs/Mb/AgNPs composite film is rapid and facile. The complex of MWNTs and AgNPs could build an electron antenna net on GCE, acting as the extending of electrode surface. Mb could form the ordered spatial orientation and arrangement on the extended electrode surface, which contributed to the rapid, reversible and efficient electron transfer of Mb.

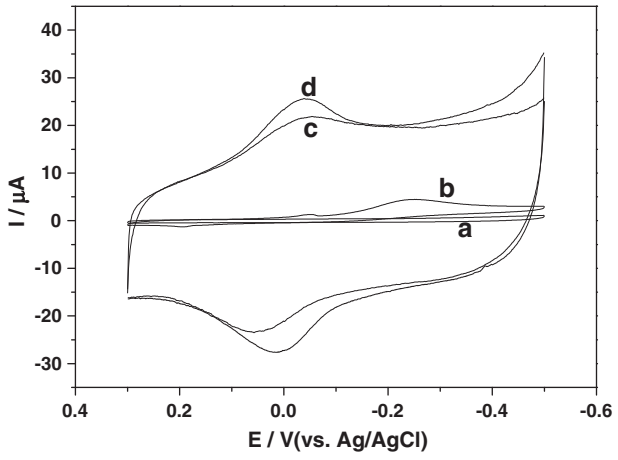


**Fig. 2.** Cyclic voltammograms of (a) bare GCE, (b) Chit-MWNTs/AgNPs/GCE, (c) Chit-MWNTs/Mb/GCE and (d) Chit-MWNTs/Mb/AgNPs/GCE in 0.1 M pH 7.0 PBS at a scan rate of 100 mV $s^{-1}$.

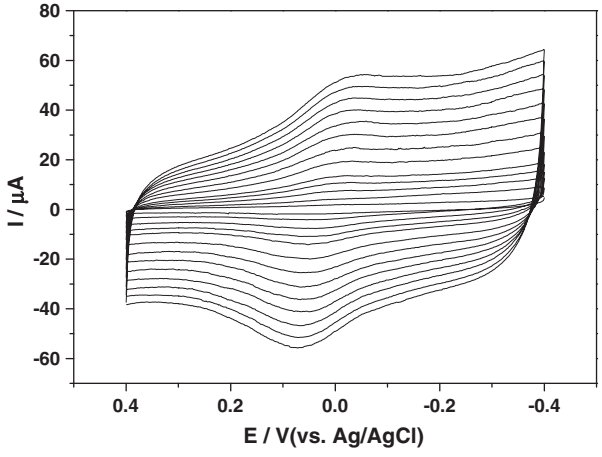


**Fig. 3.** Cyclic voltammograms of Chit-MWNTs/Mb/AgNPs/GCE in pH 7.0 PBS at 10, 25, 50, 75, 100, 150, 200, 250, 300, 350, 400, 450 and 500 mV $s^{-1}$ (from inner to outer).

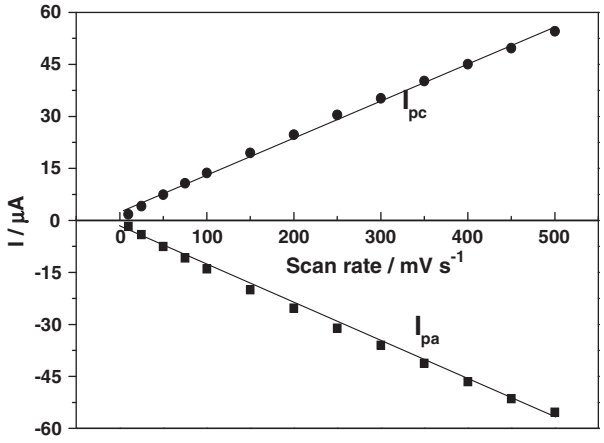


**Fig. 4.** Relationship between scan rate and the anodic and cathodic peak current of Chit-MWNTs/Mb/AgNPs/GCE in 0.1 M pH 7.0 PBS.

### 3.3. CV responses in the reduction of $H_2O_2$

Fig. 5 shows the electrocatalytic response of the Chit-MWNTs/Mb/AgNPs/GCE in the absence and presence of deoxygenated $H_2O_2$ in 0.1 M PBS of pH 7.0 at a scan rate of 100 mV $s^{-1}$. In the absence of $H_2O_2$, only the electrochemistry behavior of Chit-MWNTs/Mb/AgNPs/GCE was apparent, as a pair of reversible anodic and cathodic appeared in blank PBS. Upon addition of 0.1 M $H_2O_2$ into the electrochemical cell, the reduction peak current increased obviously while the oxidation peak current decreased, indicating a typical electrocatalytic reduction process of $H_2O_2$. The reduction current increased linearly with the concentration of $H_2O_2$ in solution, as shown in the inset of Fig. 5. That is, Mb can be recycled at the electrode during the catalytic reduction process, thus leading to a linear increase of the reduction current.

### 3.4. Selection of the applied potential

In order to obtain an efficient biosensor for $H_2O_2$, the effect of applied potential on the response of Chit-MWNTs/Mb/AgNPs/GCE was investigated. Fig. 6 shows the dependence of the amperometric current response to constant concentration $H_2O_2$ on the applied potential in the range from 0.1 V to −0.32 V (vs. Ag/AgCl). It can be seen that the response increased sharply from *ca.* 0 V to −0.3 V, reached the maximum at *ca.* −0.3 V, and then slightly decreased at more negative potentials than −0.3 V. The response of the biosensor achieved a platform when the potential arrived at −0.3 V while the current began to decrease after −0.32 V. Therefore, a constant potential of −0.3 V was adopted in order to get the maximum sensitivity, so we chose −0.3 V as the applied potential for detecting $H_2O_2$ throughout the experiment.

### 3.5. Amperometric response to hydrogen peroxide

Fig. 7 shows the amperometric response of the biosensor to the successive addition of $H_2O_2$ in 0.1 M PBS (pH 7.0) at an applied potential of −0.3 V (vs. Ag/AgCl). Consistent with the voltammetric measurement result, the biosensor showed a rapid and sensitive response to the addition of $H_2O_2$. Upon addition of an aliquot of $H_2O_2$ into the electrochemical cell, the reduction current increased rapidly to reach a stable value in less than 5 s. The response current increased with $H_2O_2$ concentration increasing, as illustrated in Fig. 7. We plotted the steady-state current vs. the concentration of $H_2O_2$. The linear relationship of the electrocatalytic reduction peak current and $H_2O_2$ concentration was obtained between $2.5\times10^{-5}$ and $2\times10^{-4}$ M, as shown in the inset of Fig. 7. The linear regression equation is I/μA = 11.77 (±0.02) + 0.042 (±0.001) $[H_2O_2]$/(M) with a correlation coefficient of 0.994 (n = 12). From the slope of calibration curve, the detection limit of $1.02\times10^{-6}$ M is estimated at S/N of 3. The analytical performance is attributed to the effective transport tunnels for small molecules in the chitosan-based composite film and the synergistic effect of MWNTs and AgNPs on electron transfer.

When the concentration of $H_2O_2$ was higher than $2.25\times10^{-4}$ M, a response plateau was observed, showing the characteristics of the Michaelis–Menten kinetic mechanism. The apparent Michaelis–Menten constant ($K^{app}{}_M$), which gives an indication of the enzyme–substrate kinetics, can be obtained from the electrochemical version of the Lineweaver–Burk equation [19]:

$$1/I_{ss} = 1/I_{max}(1 + K_M^{app}/C) \quad (2)$$

where $I_{SS}$ is the steady-state current after the addition of substrate, which can be obtained from amperometric experiments, $I_{max}$ is the maximum current under saturated substrate condition and C is the bulk concentrate of the substrate. The value of the apparent Michaelis–Menten constant ($K^{app}{}_M$) can be calculated from the slope ($K^{app}{}_M/I_{max}$) and the intercept ($1/I_{max}$) when plotting the reciprocals of the steady-state current ($1/I_{SS}$) versus the reciprocal of $H_2O_2$ concentration (1/C). Accordingly, the $K^{app}{}_M$ value for the Chit-MWNTs/Mb/AgNPs/GCE was calculated to be 0.024 mM, which is much smaller than those of

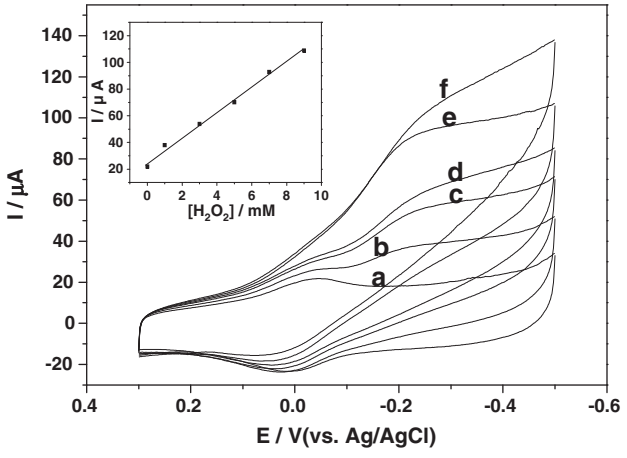


**Fig. 5.** Cyclic voltammograms of Chit-MWNTs/Mb/AgNPs/GCE in 0.1 M pH 7.0 PBS containing (a) 0 mM, (b) 1 mM, (c) 3 mM, (d) 5 mM, (e) 7 mM and (f) 9 mM $H_2O_2$. Inset: Plot of catalytic peak current vs. the concentration of $H_2O_2$.

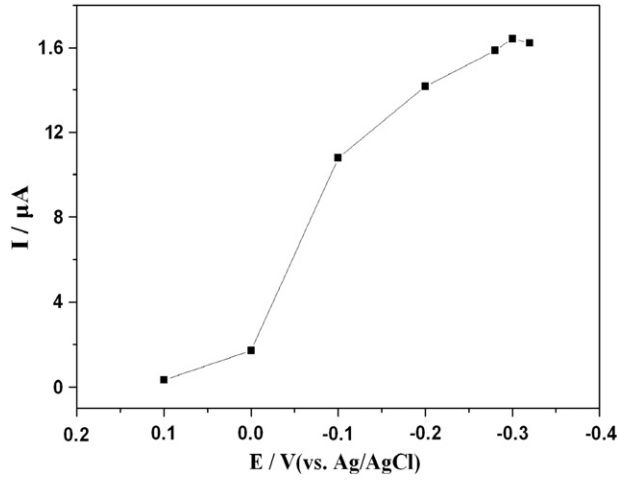


**Fig. 6.** Effect of applied potential on the response of the sensor in the presence of $2.5\times10^{-5}$ M $H_2O_2$ in 0.1 M pH 7.0 phosphate buffer solution.

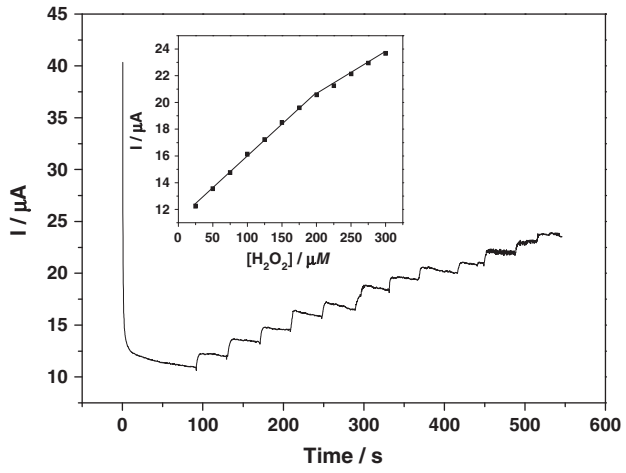


**Fig. 7.** Amperometric responses of Chit-MWNTs/Mb/AgNPs modified GCEs at −0.3 V (vs. Ag/AgCl) upon successive additions of 20 μL 6.25 mM $H_2O_2$ to 5.0 mL 0.1 M pH 7.0 PBS.

2.28 mM at cytc/Au-CPE [20], 3.69 mM at HRP-Au-CPE [21], 5.5 mM for membrane-entrapped HRP [22] and 2.3 mM for HRP/Au colloid self-assemble monolayer electrode [19]. The lower value of $K^{app}{}_M$ indicates that Mb immobilized in Chit-MWNTs/Mb/AgNPs film retains its bioactivity and has a high biological affinity to $H_2O_2$.

### *3.6. Stability and reproducibility of the hydrogen peroxide biosensor*

The stability and reproducibility of this biosensor were studied in the linear range of $H_2O_2$. After a storage period of a week in 0.1 M pH 7.0 PBS at 4 °C, the Chit-MWNTs/Mb/AgNPs modified GCE did not change the responses to $H_2O_2$. After a month, the sensor retained 95% of its initial response to $H_2O_2$. Thus, chitosan efficiently plays a role of film-forming and adhesion for the immobilization of Mb. The relative standard deviation (R.S.D) was 3.5% for six successive measurements of 6.25 mM $H_2O_2$ in 0.1 M PBS (pH 7.0), showing the proposed biosensor possesses a good reproducibility.

## 4. Conclusions

In this paper, we fabricated a biosensor by entrapping Mb/AgNPs in a composite film Chit-MWNTs on glassy carbon electrode. The nanocomposite film electrode exhibited a rapid, reversible, sensitive and stable electron transfer of Mb. The excellent performance is attributed to the large specific surface area, the effective orientation of Mb and the efficient conductivity on the complex of AgNPs and MWNTs. The proposed electrode exhibited the definite electrocatalytic response to the reduction of hydrogen peroxide and can be used as an amperometric biosensor for the determination of $H_2O_2$. The biosensor exhibited high sensitivity, good stability and reproducibility, which is ascribed to the biocompatibility and adhesion of chitosan as well as the synergistic effect of AgNPs and MWNTs on electron transfer.

## Acknowledgments

This work was supported by the Fujian Provincial Department of Education projects (JA09163) and Zhangzhou Normal University Research Fund (L20779).

## References

[1] M.K. Beissenhirtz, F.W. Scheller, F. Lisdat, A Superoxide sensor based on a multilayer cytochrome c electrode, Anal. Chem. 76 (2004) 4665–4671.
[2] M.J. Moghaddam, S. Taylor, M. Gao, S. Huang, L. Dai, M.J. McCall, Highly efficient binding of DNA on the sidewalls and tips of carbon nanotubes using photochemistry, Nano Lett. 4 (2004) 89–93.
[3] J. Huang, Z. Song, J. Li, Y. Yang, H. Shi, B. Wu, J. Anzai, T. Osa, Q. Chen, A highly sensitive L-lactate biosensor based on sol–gel film combined with multi-walled carbon nanotubes (MWCNTs) modified electrode, Mater. Sci. Eng. C 27 (2007) 29–34.
[4] B.Y. Wu, S.H. Hou, F. Yin, Z.X. Zhao, Y.Y. Wang, X.S. Wang, Q. Chen, Amperometric glucose biosensor based on multilayer films via layer-by-layer self-assembly of multi-wall carbon nanotubes, gold nanoparticles and glucose oxidase on the Pt electrode, Biosens. Bioelectron. 22 (2007) 2854–2860.
[5] K. Balasubramanian, M. Burghard, Biosensors based on carbon nanotubes, Anal. Bioanal. Chem. 385 (2006) 452–468.
[6] R. Mezzenga, J. Ruokolainen, Nanocomposites: nanoparticles in the right place, Nat. Mater. 8 (2009) 926–928.
[7] D.P. Hildebrand, H.L. Tang, Y.G. Luo, C.L. Hunter, M. Smith, G.D. Brayer, A.G. Mauk, Efficient coupled oxidation of heme by an active site variant of horse heart myoglobin, J. Am. Chem. Soc. 118 (1996) 12909–12915.
[8] S.A. Kumar, S.-M. Chen, Direct electrochemistry and electrocatalysis of myoglobin on redox-active self-assembling monolayers derived from nitroaniline modified electrode, Biosens. Bioelectron. 22 (2007) 3042–3050.
[9] C.P. You, X.W. Yan, J.L. Kong, D.Y. Zhao, B.H. Liu, Direct electrochemistry of myoglobin based on bicontinuous gyroidal mesoporous carbon matrix, Electrochem. Commun. 10 (2008) 1864–1867.
[10] B. Krajewska, Application of chitin-and chitosan-based materials for enzyme immobilizations: a review, Enzyme Microb. Technol. 35 (2004) 126–139.
[11] X. Wei, J. Cruz, W. Gorski, Integration of enzymes and electrodes: spectroscopic and electrochemical studies of chitosan–enzyme films, Anal. Chem. 74 (2002) 5039–5046.
[12] Y. Liu, X.H. Qu, H.W. Guo, H.J. Chen, B.F. Liu, S.J. Dong, Facile preparation of amperometric laccase biosensor with multifunction based on the matrix of carbon nanotubes–chitosan composite, Biosens. Bioelectron. 21 (2006) 2195–2201.
[13] Y.X. Lu, Q.F. Wang, J.Q. Sun, J.C. Shen, Selective dissolution of the silver component in colloidal Au and Ag multilayers: a facile way to prepare nanoporous gold film materials, Langmuir 21 (2005) 5179–5184.
[14] W.R. Heineman, M.L. Meckstroth, B.J. Norris, C. Su, Optically transparent thin layer electrode techniques for the study of biological redox systems, Bioelectrochem. Bioenerg. 6 (1979) 577–585.
[15] E. Laviron, General expression of the linear potential sweep voltammogram in the case of diffusionless electrochemical systems, J. Electroanal. Chem. 101 (1979) 19–28.
[16] L.Q. Rong, Z.L. Zhang, Y. Lin, Y.N. Xie, D.W. Pang, Direct electrochemistry and electrocatalysis of myoglobin entrapped in konjac glucomannan films, Chin. J. Anal. Chem. 34 (2006) 1683–1687.
[17] C.Y. Liu, J.M. Hu, Hydrogen peroxide biosensor based on the direct electrochemistry of myoglobin immobilized on silver nanoparticles doped carbon nanotubes film, Biosens. Bioelectron. 24 (2009) 2149–2154.
[18] X.J. Zhao, Z.B. Mai, X.H. Kang, Z. Dai, X.Y. Zou, Clay–chitosan–gold nanoparticle nanohybrid: preparation and application for assembly and direct electrochemistry of myoglobin, Electrochim. Acta 53 (2008) 4732–4739.
[19] R.A. Kamin, G.S. Wilson, Rotating ring-disk enzyme electrode for biocatalysis kinetic studies and characterization of the immobilized enzyme layer, Anal. Chem. 52 (1980) 1198–1205.
[20] H.X. Ju, S.Q. Liu, B. Ge, F. Lisdat, F.W. Scheller, Electrochemistry of cytochrome c immobilized on colloidal gold modified carbon paste electrodes and its electrocatalytic activity, Electroanalysis 14 (2002) 141–147.
[21] S.Q. Liu, H.X. Ju, Renewable reagentless hydrogen peroxide sensor based on direct electron transfer of horseradish peroxidase immobilized on colloidal gold-modified electrode, Anal. Biochem. 307 (2002) 110–116.
[22] T. Ferri, A. Poscia, R. Santucci, Direct electrochemistry of membrane-entrapped horseradish peroxidase. Part II: amperometric detection of hydrogen peroxide, Bioelectrochem. Bioenerg. 45 (1998) 221–226.